

# Non-gaussianity vs. non-linearity of cosmological perturbations

Licia Verde

IfA, University of Edinburgh

Royal Observatory, Blackford Hill, EH9 3HJ, Edinburgh, U.K.

Ph:+44-131-6688393; Fax:+44-131-6688416; lv@roe.ac.uk

November 6, 2018

## Abstract

Following the discovery of the cosmic microwave background, the hot big-bang model has become the standard cosmological model. In this theory, small primordial fluctuations are subsequently amplified by gravity to form the large-scale structure seen today. Different theories for unified models of particle physics, lead to different predictions for the statistical properties of the primordial fluctuations, that can be divided in two classes: gaussian and non-gaussian. Convincing evidence against or for gaussian initial conditions would rule out many scenarios and point us towards a physical theory for the origin of structures.

The statistical distribution of cosmological perturbations, as we observe them, can deviate from the gaussian distribution in several different ways. Even if perturbations start off gaussian, non-linear gravitational evolution can introduce non-gaussian features. Additionally, our knowledge of the Universe comes principally from the study of luminous material such as galaxies, but galaxies might not be faithful tracers of the underlying mass distribution. The relationship between fluctuations in the mass and in the galaxies distribution (*bias*), is often assumed to be local, but could well be non-linear. Moreover, galaxy catalogues use the redshift as third spatial coordinate: the resulting redshift-space map of the galaxy distribution is non-linearly distorted by peculiar velocities. Non-linear gravitational evolution, biasing, and redshift-space distortion introduce non-gaussianity, even in an initially gaussian fluctuation field.

I will investigate the statistical tools that allow us, in principle, to disentangle the above different effects, and the observational datasets we require to do so in practice.

## 1 Introduction

Until recently in cosmology, non-gaussianity has been a synonymous of non-linearity; but, in the last 5 years or so, more and more objects like the galaxy of [1] at redshift 5.6 have been found. For the first time a galaxy has been found at higher redshift than the most distant known quasar. More recently, a galaxy at redshift almost 7 has been found [2]. The standard “inflationary” cosmological model with gaussian initial conditions predicts that these objects should be very rare. It is becoming increasingly difficult to accommodate the existence of so many high-redshift galaxies under the assumption that non-gaussianity is equivalent to non-linearity, that is postulating gaussian initial conditions. Non-gaussianity does not necessarily imply non-linearity: there might be some primordial non-gaussianity and it is necessary to “find a way” to distinguish the two effects.

## 2 Non-gaussianity due to non-linearities

Let us start by assuming gaussian initial conditions and investigate the effects of non-linearities. We define the fractional density contrast  $\delta$  as  $\delta\rho/\rho$ , where  $\rho$  is the mean density. The probability distribution of  $\delta$  starts off symmetric around zero, with negligible tails for  $|\delta| > 1$ . Non-linear gravitational evolution skews the distribution towards high densities: this is due to the fact that underdense regions cannot become more empty than the void ( $\delta \geq -1$ ) while overdense regions can accrete matter arbitrarily (no upper limit on  $\delta$ ). This is not the only process that can skew an initially gaussian distribution. The mass in the Universe is mainly dark matter and cannot be observed directly: only galaxies can be observed, but mass and galaxy distributions may not be identical: the idea that galaxies are biased tracers of the mass distribution was introduced in the early eighties [3]<sup>1</sup> and has featured strongly in large scale structure (LSS) studies. In general, bias must alter the statistics of any underlying matter distribution, otherwise  $\delta < -1$  for the galaxy field, which corresponds to a negative galaxy density. In different bias schemes suggested in the literature, the relation between the galaxy and the mass fluctuation fields ( $\delta_g$  and  $\delta$  respectively) has been taken to be local, non-local, eulerian, lagrangian, stochastic etc...

In what follows we will assume that  $\delta_g(\mathbf{x}) = F[\delta(\mathbf{x})]$ , that is the bias, is

---

<sup>1</sup>Although the fact that galaxies of different morphologies have different spatial distributions and they cannot all be good tracers of the underlying mass distribution, was known much before the introduction of the concept of bias (e.g. [4]).

a local eulerian function of the underlying mass field. Furthermore we will assume (following [5]) that  $F$  can be expanded in Taylor series and we will truncate the expansion to the quadratic term:

$$\delta_g(\mathbf{x}) = b_0 + b_1 \delta(\mathbf{x}) + \frac{b_2}{2} \delta^2(\mathbf{x}) + \dots \quad (1)$$

$b_0$  is unimportant and simply ensures that  $\langle \delta_g \rangle = 0$ . This non-linear operation on the matter field introduces some skewness, i.e. some non-gaussianity. As first suggested by Fry [6] it is possible to disentangle the two non-gaussian contributions, non-linear gravity and bias, by looking at higher-order correlations in the mildly non-linear regime. In particular, if the initial fluctuations are gaussian and cosmological structures grow by gravitational instability, the three-point correlation function is intrinsically a second-order quantity<sup>2</sup> and is detectable in the mildly non-linear regime. If then bias can be expressed as in equation (1), it is possible to show that a likelihood analysis<sup>3</sup> of the bispectrum (the three-point correlation function in Fourier space) can yield  $b_1$  and  $b_2$ .

The bispectrum  $B(\mathbf{k}_1 \mathbf{k}_2 \mathbf{k}_3)$  is defined as

$$\langle \delta_{k_1} \delta_{k_2} \delta_{k_3} \rangle = (2\pi)^3 B(\mathbf{k}_1 \mathbf{k}_2 \mathbf{k}_3) \delta^D(\mathbf{k}_1 + \mathbf{k}_2 + \mathbf{k}_3) \quad (2)$$

where  $\delta_k$  is the Fourier transform of  $\delta(\mathbf{x})$ . Due to the presence of the Dirac delta function  $\delta^D$ , the bispectrum can be non zero only when the three  $\mathbf{k}$  form a triangle.

In practice, the higher-order statistic (the bispectrum) exploits the fact that gravitational instability skews the density field as it evolves, creating sheets and filament-like structures reminiscent of the Zeldovich pancakes. Non-linear bias also introduces skewness but does so by shifting the iso-density contours up and down, without modifying the shape of the structures. These two effects can be disentangled by using different triangle shapes for the bispectrum.

There are several advantages in performing this sort of analysis in Fourier space, most of them are the same advantages of the power spectrum over the two-point correlation function. We will recall here only the following: the estimates of power on different scales can be made uncorrelated; it is easy to deal with the error estimate; and more importantly it is easy to distinguish

---

<sup>2</sup>In the quantity  $\delta$ , assumed to be small.

<sup>3</sup>The likelihood method can easily be generalized to measure the lagrangian [7] and stochastic (e.g. [8]) bias parameters.

between linear, mildly non-linear and highly non-linear scales. In the mildly non-linear regime the bispectrum is given by:

$$\langle \delta_{g,\mathbf{k}_1} \delta_{g,\mathbf{k}_2} \delta_{g,\mathbf{k}_3} \rangle = (2\pi)^3 P_g(k_1) P_g(k_2) [c_1 J(\mathbf{k}_1, \mathbf{k}_2) + c_2] \delta^D(\mathbf{k}_1 + \mathbf{k}_2 + \mathbf{k}_3) + cyc. \quad (3)$$

where  $P_g$  denotes the galaxy power spectrum,  $J(\mathbf{k}_1, \mathbf{k}_2)$  is a known function of the two  $k$ -vectors and

$$c_1 = \frac{1}{b_1} \quad c_2 = \frac{b_2}{b_1^2}. \quad (4)$$

In the absence of bias ( $c_1 = 1$ ,  $c_2 = 0$ ) it would be easy to isolate the non-gaussianity generated by gravitational instability. Nevertheless, even in the presence of bias, it is possible to disentangle gravity from bias. Equation (3) is in a form suitable for a likelihood analysis for the two bias parameters via  $c_1$  and  $c_2$  [9], once the covariance is known<sup>4</sup>. A generating functional approach to calculate *analytically* the N-point function and therefore the covariance for the bispectrum was introduced in [10,11]. The performance of the method has been tested on biased and unbiased N-body simulations<sup>5</sup>, with very promising results<sup>6</sup> [11] for the application to forthcoming galaxy redshift surveys such as SDSS and 2dF. An estimation for the expected error achievable from present galaxy surveys, yields an error on  $c_1$  of about 100% [11] and is therefore not particularly useful.

### 3 Real world issues

Of course, reality is always more complicated: in a realistic galaxy survey several complications arise due to the presence of shot noise and selection function, but more importantly due to redshift space distortions. Galaxy surveys in fact use the redshift as the third spatial coordinate. The redshift would be an accurate distance indicator in a perfectly homogeneous Universe; but the universe is clumpy, inhomogeneities perturb the Hubble flow and introduce peculiar velocities. The resulting redshift-space map of the galaxy distribution is thus distorted along the line of sight, and the nature of this distortion is intrinsically non-linear. On large scales the coherent inflow

---

<sup>4</sup>The bispectrum is a three point quantity, its covariance is a six-point quantity (pentaspectrum).

<sup>5</sup>The N-body simulation was provided by the Hydra-consortium and produced using the code [12].

<sup>6</sup>For a different approach see J. Frieman contribution in this volume.

into overdense regions introduces a squashing effect in the redshift map (the *great wall* effect), on smaller scales, the virialized highly non-linear structures appear elongated along the line of sight (the *fingers-of-God*), heavily contaminating the mildly non-linear regime were most of the signal for the bispectrum comes from. In [13] we showed that, with an accurate modeling of redshift space distortions in the distant observer approximation, it is possible to disentangle the effects of redshift-space anisotropies from the bias and gravitational effects. This is achieved by combining a second-order perturbation theory description of the coherent inflow (e.g. [14]) with an exponential velocity dispersion model, and discarding the  $k$ -modes where the contamination from highly non-linear structures is too big to be successfully modeled. An alternative approach has also been explored (e.g. [15]).

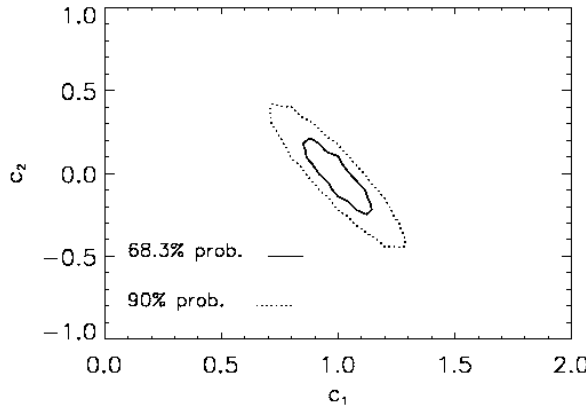


Figure 1: *Likelihood for  $c_1 = 1/b_2$  and  $c_2 = b_2/b_1^2$ , (where  $b_1$  and  $b_2$  are linear and quadratic bias parameters) for an unbiased simulation ( $b_1 = 1$ ,  $b_2 = 0$ ) in redshift space. The solid and dotted lines show the 1 and 3  $\sigma$  confidence levels respectively. This figure shows that it is possible to disentangle the non-linear gravitational instability, bias and redshift space distortion signals, and also that from future galaxy redshift surveys such as SDSS and 2dF, the bias could be known with an accuracy better than 10%.*

The result of the likelihood analysis performed on a redshift space unbiased simulation of  $100h^{-1}$  Mpc side is shown in figure 1.

It shows not only that it is possible to disentangle the non-linear gravitational instability, bias and redshift space distortion signals, but also that

from future galaxy redshift surveys such as Sloan digital sky survey (SDSS) and the Anglo-Australian two-degree field (2dF), the bias could be known with an accuracy better than 10%. Before achieving this goal however, there are several other issues to deal with, that are potentially serious for any Fourier based technique. In particular, these are the mask, the difficulty of obtaining redshifts for close pairs of galaxies, the holes arising from bright-star drills, and the variable completeness. We have investigated and quantified these effects on a simulated catalogue and concluded that a 10% error on the bias parameter could be achieved from the 2dF survey [16].

### 3.1 Bypassing the redshift-space distortions

Two-dimensional surveys avoid the redshift-space distortion problems, but, in principle, contain less information. However, because of the smaller observational effort required, these can contain a much larger number of objects. For example the APM survey at present contains  $10^6$  galaxies, the DPOSS catalogue will have 50 million galaxies and the SDSS will provide us with a two-dimensional map of  $10^7$  galaxies.

To treat the projection of higher-order correlations on the celestial sphere, the spherical nature of the distribution cannot be ignored. Spherical harmonics are eigenfunctions for the two-dimensional surface of the sphere and therefore are the natural basis describing a two-dimensional random field on the sky. When comparing with Fourier space analysis we have that

$$\delta_{\mathbf{k}} \longrightarrow a_{\ell}^m \quad (5)$$

and in particular for the bispectrum

$$\delta^D(\mathbf{k}_1 \mathbf{k}_2 \mathbf{k}_3) \longrightarrow \begin{pmatrix} \ell_1 & \ell_2 & \ell_3 \\ m_1 & m_2 & m_3 \end{pmatrix} \quad (6)$$

where on the RHS we have the three-J symbol. To perform the same sort of analysis as the one illustrated in sections 2 and 3 an expression that relates the 3D bispectrum to the projected one in spherical harmonics is needed:

$$\begin{aligned} \langle a_{\ell_1}^{m_1} a_{\ell_2}^{m_2} a_{\ell_3}^{m_3} \rangle = & \\ \begin{pmatrix} \ell_1 & \ell_2 & \ell_3 \\ m_1 & m_2 & m_3 \end{pmatrix} \left[ \frac{1}{n} \frac{16}{\pi} \sqrt{\frac{(2\ell_1+1)(2\ell_2+1)(2\ell_3+1)}{(4\pi)^3}} \times \right. & \\ \left. \int dk_1 dk_2 i^{\ell_1+\ell_2} k_1^2 k_2^2 \Psi_{\ell_1}(k_1) \Psi_{\ell_2}(k_2) \sum_{\ell\ell_6\ell_7} i^{\ell_6+\ell_7} (-1)^{\ell} B_{\ell}(k_1, k_2) (2\ell_6+1)(2\ell_7+1) \bar{\rho} \times \right. & \end{aligned} \quad (7)$$

$$\int dr r^2 \psi(r) j_{\ell_6}(k_1 r) j_{\ell_7}(k_2 r) \begin{pmatrix} \ell_1 & \ell_6 & \ell \\ 0 & 0 & 0 \end{pmatrix} \begin{pmatrix} \ell_2 & \ell_7 & \ell \\ 0 & 0 & 0 \end{pmatrix} \begin{pmatrix} \ell_3 & \ell_6 & \ell_7 \\ 0 & 0 & 0 \end{pmatrix} \begin{Bmatrix} \ell_1 & \ell_2 & \ell_3 \\ \ell_7 & \ell_6 & \ell \end{Bmatrix} + cyc. \]$$

This expression is quite complicated: the derivation and the detailed explanation of it can be found in [17]. For the purpose of this contribution we only have to notice that it is an *exact* expression relating the spherical harmonics projected bispectrum  $\langle a_{\ell_1}^{m_1} a_{\ell_2}^{m_2} a_{\ell_3}^{m_3} \rangle$  to the 3D bispectrum expressed through its Legendre coefficients  $B_{\ell}(\mathbf{k}_i \mathbf{k}_j)$ .  $\Psi_{\ell_i}(k_j)$  is a known function of the selection function,  $j_{\ell}$  denotes the spherical Bessel function and  $\{ \dots \}$  denotes the Wigner 6-J symbol.

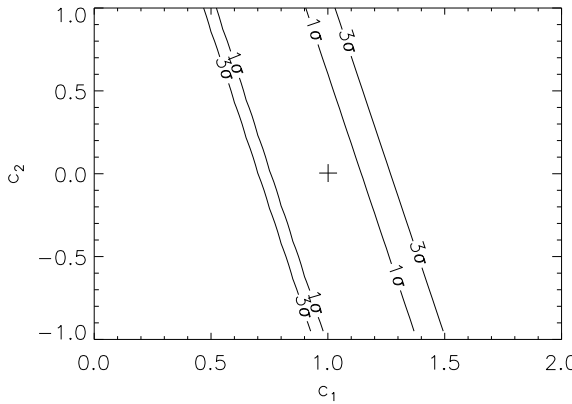


Figure 2: *Likelihood contours for degenerate triplets configurations. The two levels are the 1- $\sigma$  and 3- $\sigma$  confidence levels and the + indicates where the true value for the parameters lies. Perturbation theory breaks down at  $\ell \sim 50$ . Adding other configurations does not help much: this is about the best result obtainable from projected surveys.*

By performing a likelihood analysis to measure the bias parameter on a all sky simulation with the APM selection function, we find that the results are not encouraging for projected catalogues (see figure 2).

It is therefore preferable to undertake the bispectrum study of 3D galaxy redshift surveys such as SDSS and 2dF using the method described above. The good news is that the exact expression for the projected bispectrum in spherical harmonics has applications in a variety of areas such as cosmic microwave background (CMB) and gravitational lensing studies.

## 4 Primordial non-gaussianity: CMB vs. LSS

Up to now we have assumed gaussian initial conditions. However, among the theories for structure formation, only inflation predicts a nearly gaussian distribution for the primordial fluctuations, with deviations from gaussianity which are calculable, small and dependent on the specific inflationary model (e.g. [18,19,20]). In other models such as non-standard inflation or topological defects models initial conditions are non-gaussian. CMB and LSS data will shortly improve dramatically: it is therefore timely to ask which of the CMB or LSS will provide a better probe of the nature of primordial fluctuations. The advantage of looking at CMB maps is that the fluctuation distribution should be close to the primeval form, but the disadvantage is that the amplitude of fluctuations is small and there are foregrounds and other effects to account for. The advantages of looking at LSS is that the signal has been amplified by gravity. This is however also a disadvantage because gravity skews the distribution. Non-linear gravity, bias and redshift space distortions might completely swamp the primordial signal. Following [21], as a discriminating statistic we will use the bispectrum, but we will start by considering the skewness as an example to illustrate some of the effects.

The skewness is defined as

$$S_3 = \frac{\langle \delta^3 \rangle}{\langle \delta^2 \rangle^2}. \quad (8)$$

For a gaussian field the skewness is zero, while for an initially gaussian field evolved under gravitational instability to second order in  $\delta$ , the skewness becomes  $34/7$  and is constant in time<sup>7</sup>. In what follows for CMB related calculations, we will assume an Einstein de Sitter Universe, this assumption is justified because we shall be concerned with factors of 10 while the cosmology can change the results only by factors of order unity. Suppose the initial conditions are very close to gaussian, but with a small primordial skewness, parameterized by  $S_3(z = 1100)$  at recombination. The effect on LSS will be (e.g. [22]):

$$S_3 = S_{3,0} + 34/7 + \mathcal{F} \quad (9)$$

where  $\mathcal{F}$  includes a complicated dependence on the three- and four-point

---

<sup>7</sup>The value  $34/7$  is strictly true only for an Einstein de Sitter Universe, but the skewness does not depend strongly on cosmological parameters.

function that we will ignore for the moment and  $S_{3,0}$  scales as:

$$S_{3,0} = \frac{S_3(z)}{(1+z)} : \quad (10)$$

the primordial skewness redshifts away. We can then make a thought experiment: assume we know the real space position of every particle in the whole Hubble volume. The smallest error for the skewness, that is the smallest  $S_{3,0}$  detectable, on  $20 h^{-1}$  Mpc scales is  $S_{3,0} \sim 10^{-2}$ , which implies  $S_3(z=1100) \sim 10$ . We can repeat the exercise for the CMB where now, for consistency, we consider the smallest detectable skewness on  $0.2^\circ$  scales, obtaining  $S_3(z=1100) \sim \text{few} < 10$ .

This example already shows that CMB seems to be more sensitive to primordial deviation from gaussianity than LSS, but we will now proceed more accurately by considering the bispectrum: in fact the bispectrum contains more information than the skewness and has all the advantages of being a Fourier space quantity. In the absence of bias, the LSS bispectrum in second-order perturbation theory for non-gaussian initial condition is:

$$\begin{aligned} B(\mathbf{k}_1, \mathbf{k}_2, \mathbf{k}_3) &= B_0(\mathbf{k}_1, \mathbf{k}_2, \mathbf{k}_3) + 2J(\mathbf{k}_1, \mathbf{k}_2)P(k_1)P(k_2) + \text{cyc.} \\ &+ \int d^3k J(\mathbf{k}', \mathbf{k}_3 - \mathbf{k}') T^c(\mathbf{k}', \mathbf{k}_3 - \mathbf{k}', \mathbf{k}_1, \mathbf{k}_2) + \text{cyc.} \end{aligned} \quad (11)$$

$B_0$  is the primordial bispectrum evolved linearly and corresponds to  $S_{3,0}$  of equation 9; the second term is the usual gravitational instability bispectrum and correspond to the  $34/7$  term in equation 9;  $T^c$  denotes the Fourier counterpart of the connected four point function and the integral term correspond to  $\mathcal{F}$  of equation 9. We then parameterize the LSS bispectrum as:

$$B = P(k_1)P(k_2)[2J(\mathbf{k}_1, \mathbf{k}_2)c_1 + c_2] + \text{cyc.} \quad (12)$$

because we know how to estimate  $c_1$  and  $c_2$  from LSS studies (section 2). In the very idealized case where the real space position of every particle in the SDSS volume was known, the minimum  $c_1$  and  $c_2$  detectable would be respectively  $c_1 \sim 10^{-3}$  and  $c_2 \sim 10^{-2}$  ignoring all the real world complications of shot noise, selection function etc...

On the CMB side, the bispectrum for realistic non-gaussian models is given by (e.g. [23]):

$$B_{\ell_1 \ell_2 \ell_3} = f(\ell_1, \ell_2, \ell_3)\alpha[C_{\ell_1}C_{\ell_2} + \text{cyc.}] \quad (13)$$

where  $\alpha$  is the amplitude,  $f$  is a known function of the  $\ell$  s and  $C_{\ell}$  denotes the CMB power spectrum. The minimum error  $\sigma_{\alpha}$  on the amplitude  $\alpha$  can

be obtained via the Fisher information matrix:

$$\sigma_\alpha^{-2} = - \left\langle \frac{\partial^2 \ln \mathcal{L}}{\partial \alpha^2} \right\rangle \simeq \sum_{\ell_1 \leq \ell_2 \leq \ell_3} \frac{(B_{\ell_1 \ell_2 \ell_3} | \alpha = 1)^2}{n C_{\ell_1} C_{\ell_2} C_{\ell_3}} \sum_{m_1 m_2 m_3} \frac{\binom{\ell_1 \ell_2 \ell_3}{m_1 m_2 m_3}}{N(m_i, \ell_i)} \quad (14)$$

where  $n = 1/2$  and  $N(m_i, \ell_i)$  is the number of non-zero terms like  $C_{\ell_1} C_{\ell_2} C_{\ell_3}$  in the covariance and ranges from 1 to 30. Here we neglect partial sky coverage effects, and by constraining  $\ell \lesssim 100$  pixel noise and small angular scale effects are negligible.

In [21] we investigated the LSS and CMB bispectrum as a discriminating statistic for several physically motivated non-gaussian models. There is an infinitude of deviations from gaussianity and one cannot address them all: we thus restrict ourselves to physically motivated models where the non-gaussianity can be dialed from zero (the gaussian limit) and is assumed to be small. In particular we consider the non gaussianity parameterized by:

$$\Phi = \phi + \epsilon(\phi^2 - \langle \phi^2 \rangle) \quad (15)$$

where  $\phi$  denotes a gaussian field and for the moment we will assume that  $\Phi$  is the gravitational potential; the non-gaussianity parameter is  $\epsilon$ , that is zero for a gaussian field,  $\sim 1$  for standard inflation, but can be as big as  $\sim 20$  for some non-standard inflationary models. The CMB effect is given by  $2\epsilon/A_{SW} = \alpha$  where  $A_{SW}$  is the Sachs-Wolfe coefficient  $\sim 1/3$ .

It is possible to see [21] that, if the CMB distribution from the future satellite missions turns out to be consistent with gaussian, the smallest  $\epsilon$  allowed would be  $\sim 20$ .

The LSS effect is  $c_2 = b_2/b_1^2 + 10^{-6}\epsilon$  and the  $T^c$  contribution is negligible. By substituting the minimum  $\epsilon$  measurable from CMB in this expression and ignoring bias, we obtain  $c_2 = 10^{-4}$ : about two orders of magnitude smaller than the minimum  $c_2$  detectable from LSS even in the most idealized conditions.

In [21] also other physically motivated non-gaussian models have been considered, the result is qualitatively always the same: *if future CMB maps are consistent with the gaussian hypothesis then any non-gaussianity seen in the LSS bispectrum is due to non-linear gravity or bias*, and we know how to disentangle the two.

## 5 Looking at smaller scales

In practice, CMB studies can be affected by noise and foreground and, more importantly, there might be models in which non-gaussianity is present

mainly on LSS or galaxy scales, which are not fully accessible with CMB experiments. I will therefore investigate another two ways to detect primordial non-gaussianity on scales smaller than CMB ones.

### 5.1 Detecting non-gaussian initial conditions from large-scale structure

It is possible to bypass the contamination due to non-linear clustering and discriminate between gaussian and non-gaussian initial conditions by using higher-order statistics in LSS studies such as the trispectrum –that is the connected four-point correlation function in Fourier space [24]. This quantity has the advantage of having a rather simple growth rate, with no complicating contributions from non-linear gravity in second-order perturbation theory and that the analysis depends on cosmology and bias only through the measurable quantity<sup>8</sup>  $\beta$ . The departures from gaussian statistics can be parameterized by introducing the quantity  $H$ , which is the fractional excess of the 4-point function over the gaussian (disconnected) trispectrum. This quantity, in specific cases, can give us a meaningful measure of ‘non-gaussianity’: for mildly non-gaussian fields, a *measurement* of  $H$  can reliably be made. For highly non-gaussian fields, the gaussian hypothesis can be rejected, but the measurement of  $H$  will be unreliable. Following [24] it is possible to deal with redshift-space distortions, biasing, spatially varying selection function and shot-noise. Figure 3 shows the minimum  $\chi^2$  analysis for the parameter  $H$  from a redshift-space unbiased CDM-like simulation. By applying this method to future galaxy surveys, such as the SDSS, it will be possible to place tight constraints on initial departures from gaussian behavior.

### 5.2 The abundance of high-redshift objects as a probe of non-gaussian initial conditions

LSS probes scales much larger than galaxies but smaller than those accessible by CMB observations, and probes the present-day Universe at  $z = 0$ ; conversely CMB maps probe the Universe at redshift  $z \sim 1100$  and even larger scales. The abundance of cosmological structures at redshift in between these two ends and in particular at  $z > 1$ , contains also vital information about the nature of primordial fluctuations due to the fact that one

---

<sup>8</sup>The quantity  $\beta$  arises naturally when studying the large-scale squashing effect of structures in redshift-space maps. It is defined as  $\beta \simeq \Omega_0^{0.6}/b$  where  $b$  is the linear bias parameter.

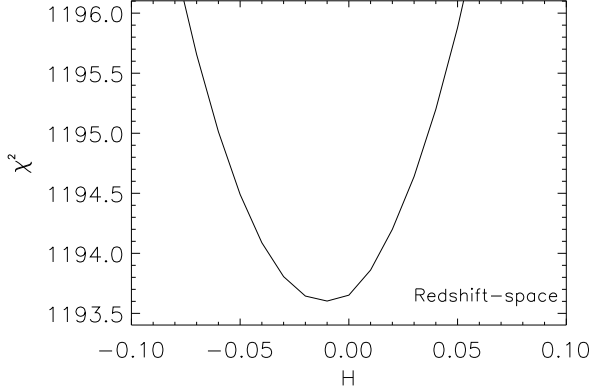


Figure 3: *Minimum  $\chi^2$  analysis for the parameter  $H$  from a redshift-space unbiased CDM-like simulation. The analysis is largely bias independent. The true value for  $H$  is 0, and it is nicely within the  $1-\sigma$  level (minimum  $\chi^2 + 0.5$ ). The quantity  $H$ , in specific cases, can give us a meaningful measure of ‘non-gaussianity’: for mildly non-gaussian fields.*

is probing the tail of the distribution. Figure 4 shows that the effect of a small non-gaussianity is dramatic on the tails: high peaks are amplified much more than low ones and deep troughs can become local maxima.

To extract this information, the Press-Schechter (PS) formalism [25] needs to be extended to non-gaussian initial conditions. The PS is an analytical model to calculate the *mass function* (that is the number of objects per unit mass at a given redshift per unit volume), within an appropriate theoretical model (see R. Sheth and S. Shandarin contributions in this volume). The key ingredient is the probability density function (PDF) for the smoothed dark matter field  $\mathcal{P}(\delta_M)$ ; in fact, the number density of objects above a given mass  $M$  (corresponding to a smoothing radius  $R$ ) at a given redshift (the *mass function*) is proportional to the quantity  $P_{>\delta_c}$ :

$$P_{>\delta_c}(\delta_M) = \int_{\delta_c}^{\infty} \mathcal{P}(\delta_M) d\delta_M \quad (16)$$

where  $\delta_c$  is the threshold overdensity for the object to collapse,  $P_{>\delta_c}(\delta_M)$  is evidently a function of the redshift of formation (or collapse) of the object  $z_c$ , this redshift dependence is enclosed in  $\delta_c$ :  $\delta_c(z) = \Delta_c/D(z)$ . Here  $D(z)$  is the linear growth factor, which in turn depends on the background cosmology,

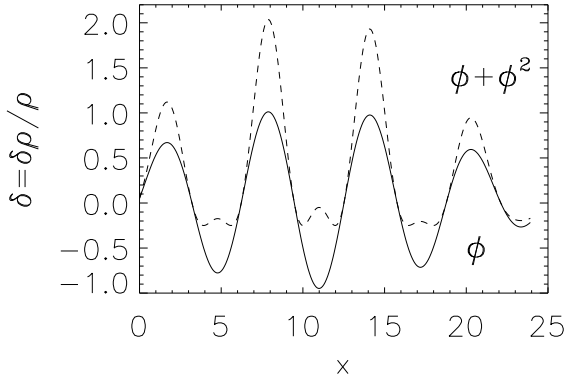


Figure 4: *The effect of a small non-gaussianity are dramatic on the tail of the distribution. Assume  $\phi$  here denotes a one dimensional gaussian fluctuation filed (black line); the dashed line is given by  $\phi + \phi^2$ . High peaks are amplified much more than low ones and deep troughs can become local maxima.*

and  $\Delta_c$  is the linear extrapolation of the overdensity for spherical collapse;  $\Delta_c$  is traditionally taken to be  $\sim 1.68$  but other values have also been used (see S. Shandarin and R. Sheth contributions).

For gaussian fields,  $\mathcal{P}(\delta_M)$  is of course well known, but needs to be computed for non-gaussian initial condition.

Given a physically motivated parameterization of primordial non gaussianity, we set off to calculate the PDF for the *smoothed* dark matter field analytically. Of course one could evaluate the PDF from numerical simulations, but this approach is plagued by the difficulty of properly accounting for the non-linear way in which resolution and finite box-size effects propagate into the statistical properties of the non-gaussian field <sup>9</sup>.

As before we parameterize the non-gaussianity as in equation 15 where  $\Phi$  can be the potential or the density field. To properly deal with the

<sup>9</sup>For example imagine computing the power spectrum of a non-gaussian field  $\psi = \phi + \phi^2 - \langle \phi^2 \rangle$  where  $\phi$  is gaussian with a power-law power spectrum  $P_\phi$ . The power spectrum of  $\psi$  involves computing the convolution of two  $P_\phi$ . This convolution is an integral over  $k$  from 0 to infinity. When performing the operation on a simulation box the final result would be as if the integral was truncated at  $k \gtrsim 2\pi/L$  and  $k \lesssim 2\pi/l$  where  $L$  is the side of the box and  $l$  is the grid resolution.

smoothing we use a path-integral approach in the calculation of the PDF:

$$\mathcal{P}(\delta_R) = \left\langle \delta^D \left[ \phi_R(x) + \epsilon \int d^3y F_R(|x-y|) \phi^2(y) - C - \delta_R(x) \right] \right\rangle \quad (17)$$

where the  $R$  subscript denotes the smoothed quantity,  $\delta^D[\dots]$  the Dirac delta function,  $\langle \dots \rangle$  the ensemble average and  $F$  is defined through its Fourier transform ( $\tilde{F}_R(k) = W_R(k)T(k)g(k)$  with  $W_R$  the smoothing,  $T$  the transfer function and  $g = 1$  for the density or  $g = -2/3(k/H_0)^2\Omega_{0,m}^{-1}$  for the potential) . In  $\phi_R$  smoothing and transfer function are easily accounted for, but in the non-gaussian part, the presence of the smoothing in  $F_R(|x-y|)$ , makes the quantity non-local. The Dirac delta function can be expressed in its integral representation and the ensemble average can be written as an integral over all  $\phi$  configurations weighted by the gaussian probability density functional. In this way we can express an unknown quantity in terms of all known quantities and we are able to obtain the non-gaussian PDF for the smoothed field analytically. The details of the derivation can be found in [26]. The main result is that, for mildly non-gaussian initial conditions with small positive skewness  $S_{3,R}$ , the threshold for collapse  $\delta_c$  is lowered, in particular [26]:

$$\delta_c(z_c) \longrightarrow \delta_c(z_c) \left[ 1 - \frac{S_{3,R}}{3} \delta_c(z_c) \right] \quad (18)$$

where  $S_{3,R}$  is directly proportional to the non-gaussianity parameter  $\epsilon$  of equation 15. By lowering the threshold for collapse rare objects will form more easily, and this has a huge impact on the tails of the distribution as shown in figures 5 and 6.

In particular figure 9 shows that the non-gaussianity of equation 15 applied to the density field with  $\epsilon \sim 10^{-4}$ , can change the number density of objects of mass  $M \sim 10^{11} M_\odot$  that collapse at redshift  $z_c = 8$ , by two orders of magnitude. Conversely, it is clear from figure 9 that non-gaussian mapping 15, applied to the potential field, has dramatic effects on cluster scales. Observations of clusters with  $z_c \gtrsim 2$  and  $M \gtrsim 10^{15} M_\odot$  could put some constraints on inflationary models [27].

### 5.2.1 A worked example

Up to date 6 galaxies with confirmed spectroscopic redshifts have been observed with redshifts  $5 < z < 7$ . The observed comoving density  $N$  is for a  $\Omega_{0,m} = 0.3$ ,  $\Lambda = 0.7$  ( $\Lambda$ CDM) Universe is  $N \geq 8.3 \times 10^{-4} (h^{-1} \text{Mpc})^{-3}$ ,  $[N \geq$

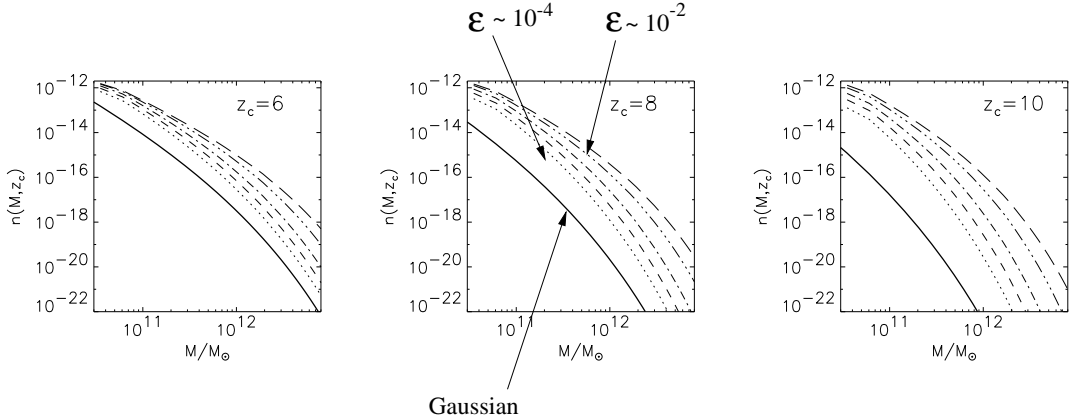


Figure 5: Effects of the non-gaussianity of equation 15 applied on the density fluctuation field. The figure shows only galaxy mass scales: the solid line is the mass function for gaussian initial conditions, all the other lines have non-gaussianity parameter  $10^{-4} \lesssim \epsilon \lesssim 10^{-2}$ . For  $z_c = 8$ , a small non-gaussianity parameter  $\epsilon \sim 10^{-4}$  increases the mass function by two orders of magnitude at about  $M \sim 10^{10} M_\odot$ .

$3.6 \times 10^{-4} (h^{-1} \text{Mpc})^{-3}$  for an Einstein-de Sitter Universe]. Their masses are very uncertain, but some estimate can be obtained with simple arguments about their observed star formation rate, these estimates can then be compared with Ly $\alpha$  width observations [26]. The gaussian  $\Lambda$ CDM model predicts  $N \geq 5.2 \times 10^{-5} (h^{-1} \text{Mpc})^{-3}$ , a factor  $\sim 20$  fewer objects, while the Einstein-de Sitter model predicts  $N \geq 10^{-7} (h^{-1} \text{Mpc})^{-3}$ : a factor  $10^4$  fewer objects! Only  $\epsilon \sim 10^{-3}$  in the density is needed to reconcile  $\Lambda$ CDM predictions with observations. Alternatively, this discrepancy could be explained postulating an error of about a factor 4 in the mass determination. As larger telescopes such as NGST get on line it will be possible to determine masses more accurately and thus constrain the amount of primordial non-gaussianity on galaxy scales.

## 6 Conclusions

We have shown that non-gaussianity does not necessarily mean non-linearity, but it is possible to distinguish different kinds of non-linearity: e.g. bias,

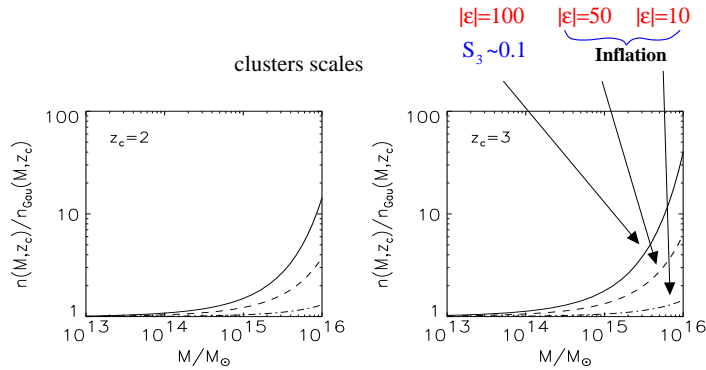


Figure 6: *The non gaussianity of equation 15 applied to the gravitational potential field has dramatic effects on cluster scales. In particular observations of clusters with  $z_c \sim 2 - 3$  and  $M > 10^{15} M_\odot$  could put constraints on inflationary models. The absolute value for  $\epsilon$  here is relatively big, but the deviation from gaussianity is still small: the skewness here is of the same order of magnitude as in figure 5.*

gravitational evolution, redshift space distortions. For the physically motivated non-gaussian models we considered, it turns out that CMB bispectrum is better than LSS bispectrum to detect primordial non-gaussianity: if the future CMB missions will produce maps that are consistent with the gaussian hypothesis, any non-gaussianity seen in the LSS bispectrum can be unambiguously attributed to the effects of non-linearities. Thus, if this is the case, from on-going LSS surveys such as SDSS and 2dF we will be able to know the bias with few % accuracy. We have also shown that, to measure the bias parameter, ongoing 3D surveys are much better than 2D ones, even with full sky coverage, but the method developed has applications in different areas such as CMB and gravitational lensing studies. To conclude, we have seen different ways to disentangle primordial non-gaussianity from effects of non-linearity: CMB bispectrum, LSS trispectrum and the abundance of high-redshift objects such as galaxies and clusters. These methods probe the Universe at different scales and at different times and in addition to that they are sensitive to different moments of the distribution. We should therefore conclude that these methods are complementary rather than mutually

exclusive.

### Acknowledgments

I would like to thank my collaborators in this work Alan Heavens, Sabino Matarrese, Marc Kamionkowski, Limin Wang and Raul Jimenez.

I also would like to thank the organizers for a very enjoyable workshop.

## References

- [1] Weymann, R. J., Stern D., Bunker A., Spinrad H., Chaffe F. H., Thompson R. I., Storrie-Lombardi L. J., 1998, *ApJLett*, **505**, L95-L98, “Keck Spectroscopy and NICMOS Photometry of a Redshift  $Z = 5.60$  Galaxy”.
- [2] Chen H. W., Lanzetta K. M., Pascarelle S., 1999, *Nature*, **398**, 586-588, “Spectroscopic identification of a galaxy at a probable redshift of  $Z = 6.68$ ”
- [3] Kaiser N, 1984, *ApJL*, **284**, L9-L12, “On the spatial correlations of Abell Clusters”.
- [4] Hubble E. P. 1938, “The realm of nebulae” New Heaven: Yale University Press
- [5] Fry N. J., Gaztanaga E., 1993, *ApJ*, **413**, 447–452, ”Biasing and hierarchical statistics in large-scale structure”
- [6] Fry N. J., 1994, *Phys. Rev. Lett.*, **73**, No.2, 215–219, ”Gravity, bias, and the galaxy three-point correlation function”
- [7] Catelan P., Lucchin F., Matarrese S., Porciani C., 1998, *MNRAS*, **297**, 692–712, “The bias field of dark matter haloes”
- [8] Taruya A., Koyama K., Soda J., 1999, *ApJ*, **510**, 541–550, “Quasi-nonlinear Evolution of Stochastic Bias”
- [9] Verde L., 1996, Large scale bias in the Universe, Laurea Thesis, University of Padua, Padua.
- [10] Verde L., Heavens A. F., Matarrese S., 1997, “Measuring  $\Omega_0$  via the bias parameter”, In *Generation of Cosmological Large-Scale structure*, D.

N. Scramm and P. Galeotti, Eds: 245-250, Nato Asi series,Dordrecht: Kluwer Academic

- [11] Matarrese S., Verde L., Heavens A. F., 1997, MNRAS, **290**, 651–662, “Large-scale bias in the Universe: bispectrum method”.
- [12] Couchman H. M. P., Thomas P. A., Pearce F. R., 1995, ApJ, **452**, 797–813, “Hydra: an Adaptive-Mesh Implementation of P 3M-SPH”
- [13] Verde L., Heavens, A. F., Matarrese S., Moscardini L., 1998, MNRAS, **300**, 747–756, “ Large-scale bias in the Universe II: redshift space distortions”
- [14] Heavens, A. F., Matarrese S., Verde L., 1998, MNRAS, **301**, 797-808, “The non-linear redshift-space power spectrum of galaxies”
- [15] Scoccimarro R. , Couchman H. M. P., Frieman J. A., ApJ, **517**, 531–540, “The Bispectrum as a Signature of Gravitational Instability in Redshift Space”
- [16] Verde L., 2000,  $\Omega_0$ , bias and primordial non-Gaussianity, Ph.D. thesis, University of Edinburgh, Edinburgh.
- [17] Verde L., Heavens A. F., Matarrese S., 2000, “Projected bispectrum in spherical harmonics and its applications to angular galaxy catalogues”, MNRAS, submitted, astro-ph/0002240
- [18] Falk T., Rangarajan R., Srednicki M., 1993, ApJLett, **403**, L1–L5, “The angular dependence of the three-point correlation function of the CMB radiation as predicted by inflationary cosmologies”
- [19] Gangui A., Lucchin F., Matarrese S., Mollerach S., 1994, ApJ, **430**, 447-456, ”The three-point correlation function of the cosmic microwave background in inflationary models”
- [20] Wang L., Kamionkowski M., 2000, Phys.Rev. D **61** 063504, “The Cosmic Microwave Background Bispectrum and Inflation”
- [21] Verde L., Wang L., Heavens A. F., Kamionkowski M., 2000, MNRAS, **313**, 141-147, “Large-scale structure, cosmic microwave background and primordial non-Gaussianity”.
- [22] Fry J. N., Sherrer R. J., 1994, ApJ, **429**, 36–42 , “Skewness in large-scale structure and non-Gaussian initial conditions”

- [23] Luo X. 1994, *ApJLett.*, **427**, L71–L74, “The angular bispectrum of the cosmic microwave background”
- [24] Verde L., Heavens A. F., 2000, “Detecting primordial non-Gaussianity from Large-scale structure”, submitted to *MNRAS*.
- [25] Press W. H., Schechter P., 1974, *ApJ*, **187**, 425–438, “Formation of Galaxies and Clusters of Galaxies by Self-Similar Gravitational Condensation”
- [26] Matarrese S., Verde L., Jimenez R., 2000, *ApJ*, **539**, “The abundance of high-redshift objects as a probe of non-gaussian initial conditions”, [astro-ph/0001366](http://arxiv.org/abs/astro-ph/0001366)
- [27] Verde et al. 2000, in preparation.